Direct quantification of surface coverage of antibody in IgG-Gold nanoparticles conjugates

Lu Zhang, David Hu, Michèle Salmain, Bo Liedberg, Souhir Boujday

Direct Quantification of Surface Coverage of Antibody in IgG-Gold Nanoparticles Conjugates

Lu Zhang,[1,2,3,4] David Hu,[1] Michèle Salmain,[2] Bo Liedberg,[3,4] and Souhir Boujday[1,4]*

[1] Sorbonne Université, CNRS, Laboratoire de Réactivité de Surface (LRS), 4 place Jussieu, F-75005 Paris, France

[2] Sorbonne Université, CNRS, Institut Parisien de Chimie Moléculaire (IPCM), 4 place Jussieu F-75005 Paris, France

[3] Centre for Biomimetic Sensor Science, School of Materials Science and Engineering, Nanyang Technological University, 637553 Singapore

[4] MajuLab, UMI 3654, CNRS-UNS-NUS-NTU International Joint Research Unit, Nanyang, Singapore

Laboratoire de Réactivité de Surface, UMR CNRS 7197, *Sorbonne Université*, case 178, 4 Place Jussieu, 75252 Paris cedex 05, France

Tel: +33144276001, Fax: +33144276033, souhir.boujday@sorbonne-universite.fr

Highlights

- Antibody surface coverage on gold nanoparticles is measured by fluorescence-based assay
- The direct assay gives more reliable results than indirect fluorescence assay or ELISA
- Physisorption and chemisorption to gold nanoparticles give the same antibody coverage
- Adsorbed antibody retains good immunoreactivity

Declarations of interest: none

ABSTRACT

It is of paramount importance to be able to accurately quantify surface coverage of antibodies on gold nanoparticles (AuNP) so as to optimize the sensitivity of AuNP-based immunosensors. Herein, we developed a fluorescence-based method to directly quantify rabbit immunoglobulin G (IgG) used as antibody model bound to AuNP. Rabbit IgG was first labelled with fluorescein-5-isothiocyanate (FITC) prior to conjugation to AuNP *via* either physisorption or chemisorption. IgG-conjugated AuNP were treated with NaCN to dissolve the AuNP and restore the fluorescence emission that was quenched in the presence of the metallic colloids, followed by quantification of fluorescein by spectrofluorimetry. This direct assay gave about 4 IgG bound to each 15-nm diameter AuNP for both immobilization strategies. This surface coverage value was in good agreement with that determined from the theoretical value calculated from the Localized Surface Plasmon Resonance (LSPR) band shift. For comparison, we also applied two indirect quantification methods based on the quantitation of excess IgG remaining in the supernatant using fluorescence assay or enzyme-linked immunosorbent assay (ELISA). The indirect assays, either fluorescence or ELISA, commonly used to assess the antibody coverage on AuNP, overestimated the IgG surface coverage to a large extent, since up to 3 to 4 times higher coverages were measured. Therefore, the direct fluorescence method reported in this paper appears as a valuable method for quantification of surface coverage of antibody on AuNP.

KEYWORDS. Gold nanoparticles, immunoglobulin G (IgG), quantification, fluorescence, adsorption.

1. INTRODUCTION

Antibody-modified gold nanoparticles (AuNP) are widely used in optical biosensing technologies [1-10]. The performance of AuNP-based biosensors is markedly dependent on the conjugation chemistry between antibody (Ab) and AuNP that in turn controls surface coverage and antibody orientation [11-15]. In order to optimise the surface coupling chemistry and thereby the assay sensitivity, a reliable method to determine antibody surface coverage is highly desirable.

Several quantitative methods to measure surface coverage of antibodies conjugated to AuNP have been reported to date. Generally, the quantity of adsorbed antibody, and thus the surface coverage, is indirectly deduced from the amount of unbound antibody remaining in the supernatant after adsorption to AuNP. It can be performed by the classical colorimetric Bicinchoninic Acid (BCA) or Bradford protein assays [16-19]. However, antibody quantification by these indirect methods often leads to overestimation of antibody surface coverage on AuNP. Moreover, when a blocking step with another protein, typically BSA, is performed to prevent aggregation of the nanoparticles in saline environment as well as to increase the long-term stability of the Ab-AuNP conjugates [20], this approach becomes inapplicable. In this case, unbound antibody can be quantified by ELISA using a microtiter plate coated with the corresponding antigen [2].

Direct methods for the quantification of antibody in AuNP conjugates have also been reported, like the BCA protein assay [21]. However, despite careful calibration treatment, *i.e.* removal of nanoparticles contribution by subtracting the absorbance of the AuNP, antibody concentration was still overestimated. To circumvent the interference from nanoparticles, dissociation of antibody from nanoparticles prior to quantification was also performed. For example, dissolution of the Ab-AuNP conjugate was achieved with KI/I_2 mixture, followed by labeling of recovered antibody by the fluorescent dye NanoOrange and spectrofluorimetric measurement [19]. Although this method gave more reliable results than indirect protein assay methods, it is still not applicable to Ab-conjugated AuNP that are subsequently blocked by BSA. Similarly, the amount of a protein conjugated to AuNP was measured by complete digestion in 6 N HCl followed by fluorescent labeling of the generated aminoacids and assay of glycine by HPLC coupled with fluorescence detection [22, 23]. Alternatively, antibody coverage was quantified by ELISA using the corresponding antigen labeled by HRP [11, 18].

Antibody coverage to AuNP can also be quantified from the LSPR peak shift caused by antibody-induced changes in the local refractive index (RI) [24, 25]. Though this approach provides a direct quantification of the adsorbed antibody, it requires accurate knowledge of proteins' RI at the nanoparticles surface which in turn depends on the surface coverage, protein orientation and water content [26-28].

Interestingly, surface coverage of DNA on AuNP has been previously quantified by a fluorescence-based method involving fluorescently-labeled DNA strands. Its principle is based on the displacement of DNA strands chemisorbed on AuNP by mercaptoethanol or by nanoparticle dissolution in KCN followed by spectrofluorimetric measurement [29]. Such a strategy could be translated to antibody-AuNP conjugates using fluorescently labeled antibody. Since the antibody is labeled by the fluorophore prior to AuNP adsorption, only the adsorbed antibody and not the other proteins will be eventually quantified.

In this paper, we wish to report the implementation of a fluorescence-based method for the direct determination of surface coverage of a model antibody, namely rabbit IgG, on spherical AuNP. FITC-labeled IgG (FITC = fluorescein-5-isothiocyanate) is first conjugated to AuNP. Then the AuNP conjugates are dissolved by NaCN to release FITC-labelled IgG [30, 31] which is subsequently assayed using spectrofluorimetry. This direct method is benchmarked against two indirect methods that rely on assay of excess FITC-labelled IgG in the supernatant using spectrofluorimetry or sandwich ELISA. This quantification method was successfully applied to IgG-AuNP bioconjugates resulting from physisorption of IgG on AuNP or chemisorption via sulfur-gold bonds.

2. MATERIAL AND METHODS

2.1. Material

Gold(III) chloride trihydrate (99.9%), sodium citrate dihydrate, tannic acid, 2-iminothiolane hydrochloride (Traut's reagent), bovine serum albumin (BSA), rabbit IgG (I-5006), goat anti-rabbit IgG (R-5001), fluorescein-5-isothiocyanate (FITC), HRP conjugated goat anti-rabbit IgG (A-6154) were purchased from Sigma-Aldrich. Phosphate-buffered saline (PBS) (pH = 7.4) was obtained from Fisher. Milli-Q water (18 MΩ·cm, Millipore) was used for the preparation of aqueous solutions.

2.2. Gold nanoparticle synthesis

Colloidal spherical AuNP were prepared according to the Slot & Geuze method [32]. Two stock solutions were firstly prepared: solution A, 1 mL of 1% (w/v) $HAuCl_4$ and 79 mL of deionized water; solution B, 4 mL of 1% sodium citrate, 0.025 mL of 1% tannic acid, and 16 mL of deionized water. Solutions A and B were heated to 60 °C and mixed while stirring. Then the mixture was heated up to 90 °C, once the solution turned red. The temperature was increased until boiling and kept under reflux for 30 min. Finally, the solution was cooled on ice bath and stored in a light-proof container at 4 °C. The colloidal solution of AuNP was characterized by UV-Vis spectroscopy, dynamic light scattering (DLS), zeta potential and transmission electron microscopy (TEM).

2.3. Chemical modification of IgG

2.3.1. FITC labeling of IgG

To a solution of rabbit IgG (2 mg/mL in 0.1 M sodium carbonate buffer, pH 9, 500 µL), was slowly added a solution of FITC (1 mg/mL in anhydrous DMSO, 25 µL) while gently and continuously stirring the protein solution. The reaction mixture was incubated overnight at 4°C in the dark. A solution of NH_4Cl (2 M, 12.5 µL) was added to a final concentration of 50 mM and incubated for 2 h at 4 °C, to quench the reaction. Then glycerol (25 µL) was added to a final concentration of 5% (v/v). Unbound FITC was separated from the IgG(FITC) conjugate by diafiltration in PBS using an Amicon Ultracentrifugal filter (30 kDa cutoff). The concentration of FITC in filtrates after each centrifugation was quantified by reading the absorbance at 495 nm. Cycles of concentration/dilution were repeated until the concentration of FITC in filtrates no longer decreased. The IgG(FITC) conjugate was recovered and stored in a light-proof container at -20°C. IgG concentration of IgG(FITC) sample was determined from the absorbance at 280 nm (A_{280}) and the absorbance at 495 nm (A_{495}) according to equation 1

$$IgG\left(\frac{mg}{ml}\right) = \frac{A_{280} - 0.35 * A_{495}}{1.4} \qquad \text{Equation 1}$$

Where 1.4 is the A_{280} of IgG at a concentration of 1.0 mg/mL at pH 7.0, and ($0.35 \times A_{495}$) is the correction factor due to the absorbance of FITC at 280 nm. The F/P ratio is defined as the number of Fluorescein entities (F) per molecule of IgG (P stands for Protein) in the conjugate. It was calculated according to equation 2

$$\frac{F}{P} = \frac{2.77 * A_{495}}{A_{280} - 0.35 * A_{495}}$$ Equation 2

2.3.2. Thiolation of IgG(FITC)

Traut's reagent (1 mg/mL, 40 equiv.) was allowed to react with IgG(FITC) in 40 mM phosphate buffer, pH 8.0 for 1 h at room temperature to generate sulfhydryl groups [33]. The thiolated IgG(FITC)-SH was separated from excess Traut's reagent by gel filtration (Dextran desalt column, 10 mL, Thermo Fisher) using 10 mM phosphate buffer, pH 7.4 (PB) as eluent. One-ml fractions were collected and analyzed at 280 nm. The fractions containing the protein were pooled and the resulting IgG(FITC)-SH solution was concentrated by ultrafiltration using a centrifugal filter (Amicon ultra-4, 50 kDa cutoff, Millipore).

2.4. Conjugation of IgG to gold nanoparticles

For chemisorption of IgG to AuNP, the colloidal AuNP solution (5 mL, 14.8 ± 1 nm diameter) was adjusted to pH 8 - 9 with K_2CO_3 solution (0.1 M), followed by addition of 55 µg of IgG(FITC)-SH (in PB). The solution was incubated for 1 h at room temperature, then BSA was added to a final concentration of 0.5% (w/v) to block the free binding sites on the AuNP. After another 1 h, the solution was centrifuged at 10,000g for 30 min at 4°C and the supernatant (S1 in Fig. S2) was retrieved and re-centrifuged to give S1a that was kept for analysis (Fig. S2). The first (P1) and second (P1a) pellets were pooled and redispersed in PB supplemented with 0.25% BSA (w/v) (5 mL). The solution was submitted to a second round of centrifugation and the resulting pellet was finally re-dispersed in storage buffer (0.25% BSA (w/v) in PB, 4 mL) while the supernatant (S2a, Fig. S2) was kept for analysis. The final conjugate is named AuNP-S-IgG(FITC). Physisorption of IgG(FITC) or BSA to AuNP was carried out according to the same protocol using IgG(FITC) or BSA and the final conjugates are named AuNP-IgG(FITC) and AuNP-BSA, respectively.

2.5. Dissolution of IgG-conjugated AuNP

AuNP or IgG(FITC)-conjugated AuNP (500 µL) were mixed with NaCN (1 mg/mL adjusted to pH 12 with NaOH, 325 µL) and incubated overnight. Complete dissolution of the nanoparticles was evidenced by the disappearance of the LSPR peak of AuNP (Fig. S5).

2.6. Quantification by spectrofluorimetry

Quantification of fluorescein in the supernatants S1a and S2a and in the bioconjugates after dissolution of nanoparticles according to the above procedure was done by spectrofluorimetry. Fluorescent signal is highly sensitive to medium change. In order to build up accurate calibration curves, standard solutions were prepared in the same matrix as the samples. The appropriate steps performed to match the matrix are given in the supplementary part and illustrated in Fig. S6 and the calibration curves are shown in Fig. S7-9.

2.7. Quantification of excess IgG by ELISA

Goat anti-rabbit IgG (10 µg/mL in carbonate buffer, pH 9.5, 100 µL) was pipetted into each well of a flat-bottomed polystyrene 96-well plate (Greiner bio-one) and incubated overnight at 4°C. The content was discarded and non-specific sites were blocked by PBS-0.1% BSA (100 µL) for 1 h at room temperature. Wells were washed 3 times with PBS-0.05% Tween 20. Standard solutions of IgG(FITC) or samples (100 µL in duplicate) to be quantified were dispensed into the wells. The plate was incubated 2 h at room temperature. After washing with PBS-0.05% Tween 20 (3x100 µL), HRP-labelled goat anti-rabbit IgG conjugate (1/4000, 100 µL) was added to each well and incubated 1 h at room temperature. After washing with PBS-0.05% Tween 20, a mixture of o-phenylenediamine dihydrochloride (OPD) and H_2O_2 (7 mg OPD + 4 µL H_2O_2 in 10 mL of citrate-phosphate buffer, pH 5, 100 µL) substrate solution was added to each well. After the color developed, H_2SO_4 (2.5 M, 50 µL) was added to each well to stop the enzymatic reaction. After 10 min in the dark, the absorbance of each well was read at 485 nm with a microplate reader (Fluostar Optima, BMG Labtech). The concentration of IgG(FITC) or IgG(FITC)-SH in the samples was deduced from the calibration curve established by plotting A_{485} vs. IgG(FITC) concentration (Fig. S11).

2.8. Immunoreactivity of IgG conjugated to AuNP

HRP-conjugated goat anti-rabbit IgG (10 µL, 0.45 mg/ml) was added AuNP-S-IgG(FITC), AuNP-IgG(FITC) or AuNP-BSA colloidal suspension (500 µL) and the mixture was incubated for 30 min. Excess HRP-anti-IgG conjugate was removed by repeated cycles of centrifugation (10 000 g; 30 min; 4°C) and resuspension in storage buffer (500 µL) until the supernatant showed no colour upon addition of OPD and H_2O_2. The final AuNP pellet was resuspended in storage buffer (500 µL) and a 1:100 dilution was made in storage buffer. The solution (100 µL/well in duplicate) was dispensed in a 96-well microtiter plate and the mixture of OPD and H_2O_2 was added (100 µL/well). After exactly 3 min, the enzymatic reaction was stopped by adding H_2SO_4 (2.5 M; 50 µL/well) and the absorbance at 485 nm was

read after 10 min in the dark as above. A calibration curve was established from solutions of HRP-anti-IgG in storage buffer. The concentration of AuNP was determined by measuring the absorbance of the AuNP suspensions at 520 nm taking an extinction coefficient of $3.8x10^8$ $M^{-1}.cm^{-1}$.

2.9. Characterization techniques

UV-Visible (***UV-Vis***) spectra were acquired on a Cary 50 spectrophotometer (Varian, Inc.). Analysis of colloidal solutions was performed in the range 300 - 800 nm. Protein solutions were analyzed at 280 nm and 495 nm (for FITC). Milli-Q H_2O was used as the blank. Dynamic light scattering (***DLS***), and zeta potential (***ELS***) measurements were performed using Litesizer™ 500 apparatus (Anton Paar) equipped with a 658 nm laser operating at 40 mW. The backscattered light collection angle was set to 90°. The zeta potential was measured in a Ω-shaped capillary tube cuvette with an applied potential of 150 V. AuNP were visualized using a JEOL JEM 1011 transmission electron microscope (***TEM***) operating at an accelerating voltage of 100 kV. A drop of AuNP colloidal solution was dispensed on a carbon-coated copper grid and dried at room temperature before imagining. The size distribution of AuNP was determined using Image J. ***Fluorescence*** spectra were acquired with a FP-6200 spectrofluorimeter (Jasco) using a 1-cm pathlength quartz cuvette. The bandwidth of emission/excitation is 5 nm/5nm. Excitation was set at 485 nm and emission was measured in the range of 495 nm to 600 nm with a scanning speed of 250 nm/min. Temperature was controlled by a Peltier element and set at 20 ± 0.1 °C.

3. RESULTS AND DISCUSSION

3.1. Gold nanoparticle synthesis and characterization

As synthesized AuNP were characterized by UV-visible spectroscopy, transmission electron microscopy (TEM), dynamic light scattering (DLS) and zeta potential measurements. The absorption spectrum exhibits a distinct plasmon peak at ~520 nm (Figure 1-A), corresponding to spherical AuNP with a narrow distribution in size and shape. This observation is confirmed by TEM images (Figure 1-C and D). The size distribution taken by analyzing ca. 1000 particles is narrow (Figure 1-B) and the average size of AuNP is centered at 14.8 ± 1 nm obtained by Gaussian distribution. The concentration of AuNP solution was equal to 2.8 nM using an extinction coefficient of 3.8×10^8 M^{-1} cm^{-1} taken from the literature [34]. The

colloidal solution was further characterized using DLS and zeta potential measurements. Hydrodynamic diameter (intensity weighted peak) of AuNP is 20.9 nm with polydispersity of 0.12, and the mean zeta potential is -55.75 ± 2.5 mV.

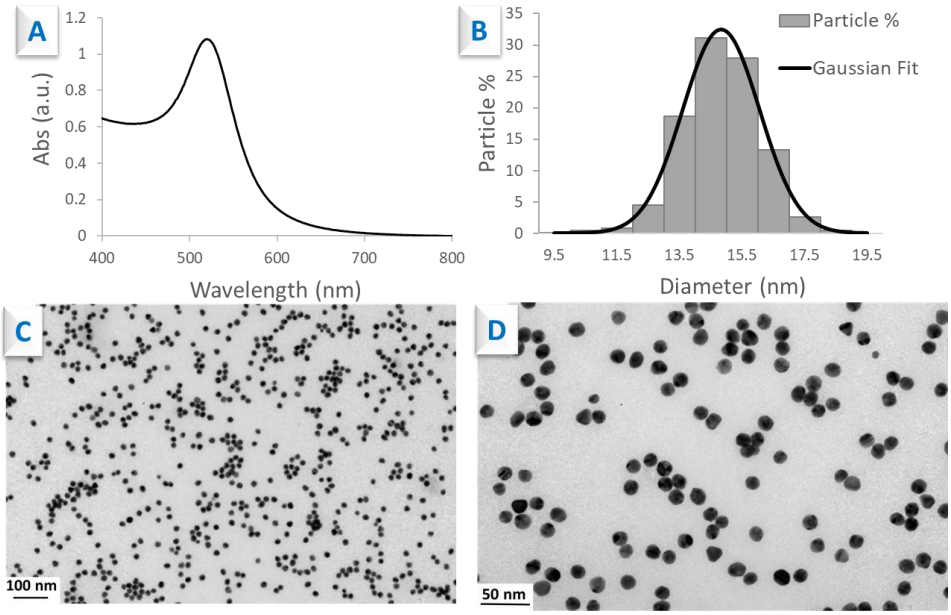

Figure 1 : Characterization of AuNP: A. UV-Vis absorption spectrum of colloidal AuNP solution, B. histogram of AuNP size distribution; C. and D. TEM images of AuNP.

3.2. Chemical modification of IgG

Labeling of rabbit IgG by FITC was done according to Figure 2-A to yield an IgG(FITC) conjugate with a F/P ratio of 1.9 (Fig. S1 and Table S1). IgG(FITC) was used as such for physisorption to AuNP. Alternatively, since rabbit IgG does not contain any free cysteines, thiol functions were chemically introduced via the lysine amino groups using Traut's reagent to produce IgG(FITC)-SH (Figure 2-B). This thiolated bioconjugate was then used for chemisorption to AuNP by formation of S-Au bonds. Surprisingly, the calculated F/P ratio of IgG(FITC)-SH is 1.34. (Table S1) The decrease of F/P may be due to the additional diafiltration steps performed after thiolation that may have further removed weakly bound FITC.

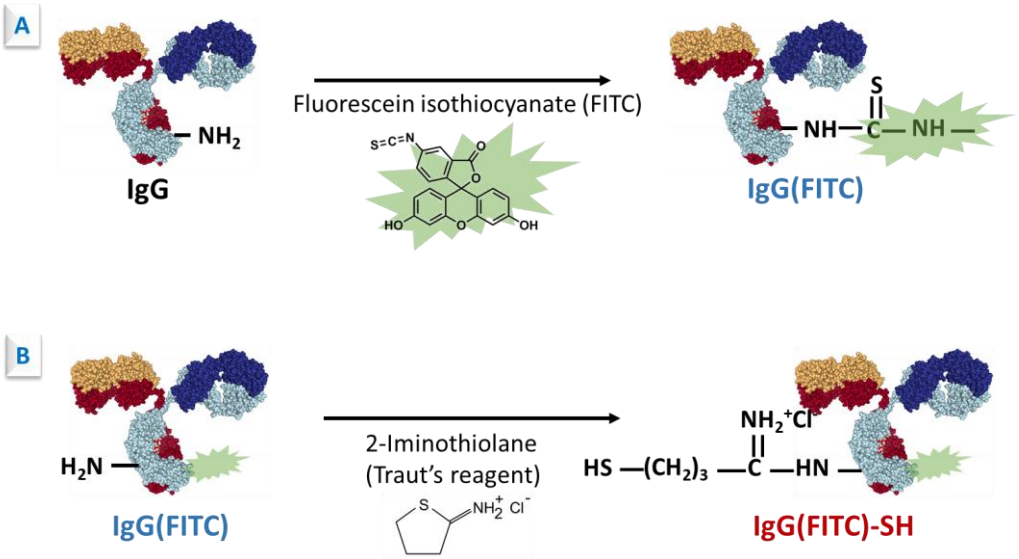

Figure 2 : Schematic illustration of chemical modification of IgG: A. FITC labelling of IgG; B. thiolation of IgG(FITC).

3.3. Engineering of IgG(FITC)-AuNP bioconjugates

Stepwise conjugation of IgG(FITC)-SH to AuNP was characterized by absorption spectroscopy. Figure 3-A shows the absorption spectrum of the colloidal solution of AuNP before and after chemisorption of IgG(FITC)-SH. The position of the LSPR peak was determined from the zero value of the first derivative of spectrum shown in Figure 3-C as recommended in the literature [35]. The LSPR peak of AuNP initially at 519 nm (black trace) shifted to 522 nm (red trace) after 1 h incubation, as a result of chemisorption of IgG(FITC)-SH on the AuNP. Addition of BSA to block the free binding sites led to a further shift of the LSPR peak to 526 nm (not shown). The final AuNP-S-IgG conjugate was re-analyzed after centrifugation and re-suspension in storage buffer and its LSPR peak appeared at 527 nm (dark cyan trace). The LSPR peak of AuNP after physisorption of IgG(FITC) and BSA blocking step followed the same trend, as shown in Figure 3–B and D. We noticed that LSPR peak shift for the IgG adsorption step (i.e. 3 nm, for both chemisorption and physisorption) was smaller than that of native IgG on AuNP (Fig. S3 ~5 nm). The UV-Vis spectrum of IgG(FITC) (Fig. S1) displays a peak at 495 nm owing to the contribution of FITC that is quite close to that of AuNP. Its presence interferes with the peak of AuNP, by counterbalancing the red shift due to antibody adsorption, thus leading to an overall smaller peak shift after adsorption of IgG(FITC).

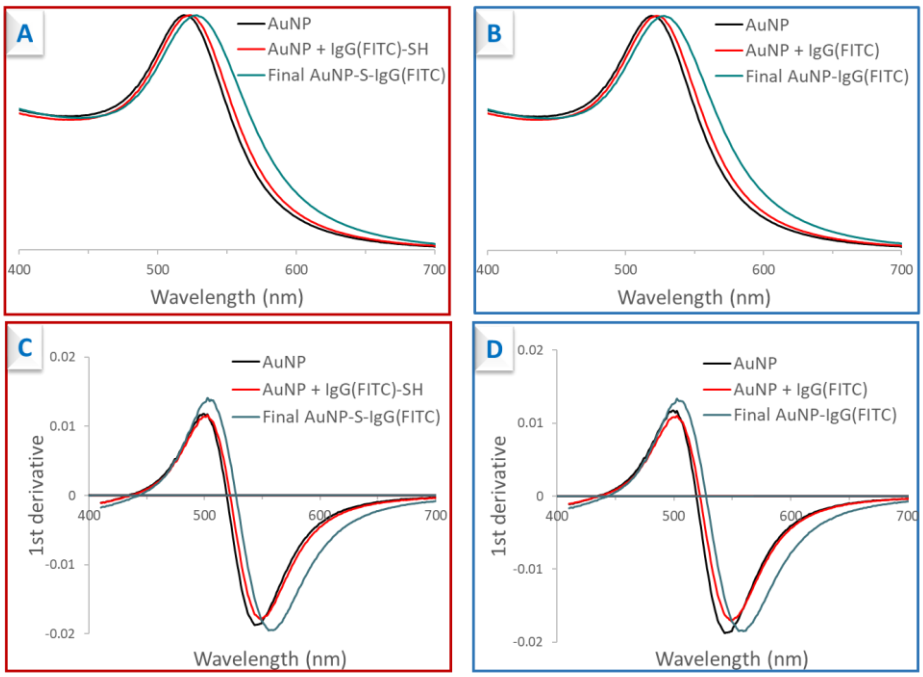

Figure 3 : Normalized UV-Vis absorption spectra of A. chemisorption and B. physisorption of IgG(FITC)-SH and IgG(FITC) on AuNP. First order derivative of UV-Vis absorption spectra in A and B are shown in C. and D.

Dynamic light scattering (DLS) and zeta potential measurements were performed on the colloidal solution before and after conjugation, in order to check the changes in the hydrodynamic diameter (D_H) and the zeta potential due to the adsorption of IgG(FITC) to AuNP. The results are summarized in Table 1. Chemisorption of IgG(FITC)-SH followed by BSA blocking step induced a large increase of the D_H of nanoparticles from 20.9 nm to 101.9 nm while physisorption of IgG(FITC) resulted in an increase of D_H to 120.4 nm. Let us note that a large amount of BSA was used at the blocking step (0.5% (w/v)) and that the final storage buffer also contains a large amount of BSA (0.25% (w/v)). We can reasonably suppose that a multilayer of BSA molecules formed on top of the layer of IgG molecules is responsible for the large increase of D_H [19]. The zeta potential increased from -55.8 mV to -15.7 mV for AuNP-S-IgG(FITC) and -18.3 mV for the AuNP-IgG(FITC) conjugate. On the other hand, the net charge of the bioconjugates is expected to be close to that of the protein itself at the working pH, if the protein fully covers the surface of AuNP. Here as AuNP surface is covered by a mixture of IgG and BSA. The zeta potential of rabbit IgG is -16.1 mV [2] and we measured the zeta potential of BSA which is -10.9 mV at pH 7.4. The zeta

potential of the bioconjugates measured here is in agreement with the values for rabbit IgG and BSA.

Table 1 : Hydrodynamic diameter and zeta potential of AuNP and IgG-conjugated AuNP.

Nanoparticles	D_H (nm)	Polydispersity	Mean zeta potential (mV)
AuNP	20.9	0.12	-55.8 ± 2.6
AuNP-S-IgG	101.9	0.24	-15.7 ± 0.7
AuNP-IgG	120.4	0.28	-18.3 ± 0.6

3.4. Quantification of surface coverage by fluorescence spectrometry

FITC-based fluorescence assay was set up to quantify IgG adsorbed on AuNP. Not surprisingly, once adsorbed on AuNP, the emission of fluorescein entities of Ig(FITC) was mostly quenched (Figure 4) [36, 37]. To recover the FITC fluorescence emission, the AuNP had to be dissolved by NaCN. Complete dissolution of the IgG-conjugated nanoparticles was assessed by the disappearance of the LSPR peak of AuNP (Fig. S5). Subsequent release of IgG(FITC) restored the fluorescence emission of fluorescein entities bound to IgG which was detected and quantified by spectrofluorimetry (Figure 4). The concentration of IgG(FITC) was calculated according to the related calibration equation (Table S3). The concentration of AuNP in the bioconjugate was calculated from the optical density of the colloidal solution at 527 nm (before cyanidation) assuming the same extinction coefficient as the citrate-coated AuNP ($\varepsilon = 3.8 \times 10^8\ M^{-1}.cm^{-1}$). An antibody surface coverage of 3.9 or 4.3 IgG per AuNP was calculated for the AuNP-S-IgG and AuNP-IgG conjugates, respectively. The surface coverage of IgG immobilized via chemisorption did not differ significantly from the surface coverage resulting from physisorption of IgG to AuNP.

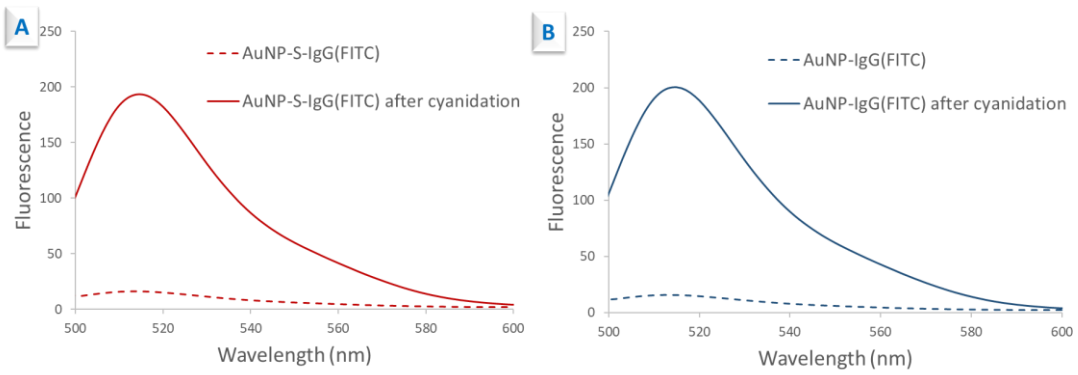

Figure 4 : Fluorescence emission spectra of IgG-AuNP conjugates before and after cyanidation.

3.5. Indirect quantification of surface coverage

3.5.1. By fluorimetry

The concentration of excess IgG(FITC) in the supernatants S1a and S2a collected after both washing steps was also measured using fluorescein emission and the related calibration equations listed in Table S3. The quantity of IgG(FITC) bound to the AuNP was assumed to be the difference between added IgG(FITC) and the unbound IgG(FITC) present in both supernatants. As a result, the antibody coverage was found equal to 13.3 IgG per AuNP for AuNP-S-IgG and 15 IgG per AuNP for AuNP-IgG. These values are much higher than those measured by the direct fluorescence-based method.

3.5.2. By ELISA

In the process of cyanidation at basic pH, both inter-chain and intra-chain disulfide bonds of IgG are cleaved by cyanide, followed by elimination of thiocyanate ions [38]. The alkali solution also leads to the degradation of IgG [39]. Both effects led to the denaturation of IgG that prevented its quantification by ELISA. So ELISA was only used to quantify excess IgG in supernatants S1a and S2a. The calibration curve of IgG concentration is shown in Fig. S11. After subtracting the quantity of IgG in supernatants, surface coverages of 6.9 IgG per AuNP for AuNP-S-IgG and 9.9 IgG per AuNP for AuNP-IgG were calculated. Again the coverages are substantially higher than those calculated by the direct method.

The bar chart in Figure 5 gathers the experimental surface coverages of IgG determined by the three methods. For comparison, the monolayer surface coverage of IgG on 14.8-nm diameter spherical gold nanoparticles theoretically estimated from the surface area of one nanoparticle and the average footprint of one antibody was calculated to be 9.8 IgG per nanoparticle (see Appendix). We also evaluated the surface coverage from the LSPR peak shift consecutive to adsorption of native IgG to AuNP (Fig. S3) that gave a value of 3.9 IgG per AuNP (see detailed calculations in Appendix). This value is in very good agreement with the fluorescence-based direct method to quantify antibody coverage.

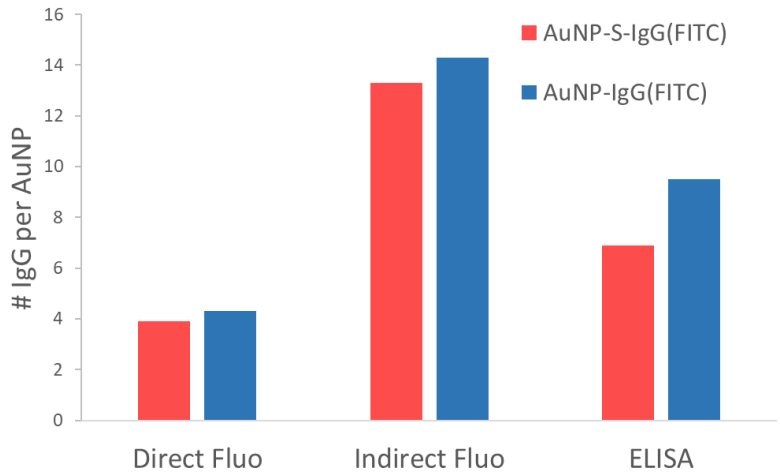

Figure 5 : Surface coverages of IgG adsorbed on AuNP measured by direct fluorescence-based assay of IgG(FITC) released from the AuNP conjugates (direct Fluo), indirect fluorescence assay (indirect Fluo) and ELISA by analysis of unbound IgG(FITC) in the supernatants.

Experimentally, the direct fluorescence assay gave around 4 IgG per AuNP for both AuNP-S-IgG and AuNP-IgG, which is in agreement with the calculation according to LSPR band shift, but lower than the theoretical value of 9.8 calculated from the IgG footprint assuming equal probability of IgG orientations on AuNP. We then compared surface coverages of differently oriented IgG on AuNP (Fig. S4 and Table S2) and we found the value obtained from 'flat-on' mode is very close to the direct fluorescence assay result. With this mode, the contact surface between IgG and AuNP is maximized, leading to stronger electrostatic interactions between IgG and AuNP, therefore, better stability of conjugates. For chemisorption, electrostatic interactions between IgG and AuNP may still predominant even in the presence of S-Au bonds. The indirect fluorescence assay gave 13.3 or 15 IgG per AuNP, this overestimation may be partially due to the loss of IgG in the washing steps. Errors in the estimation of IgG(FITC) concentration may also arise from the fluorescence measurements themselves since, as mentioned above, emission of fluorescein is highly sensitive to the medium. Indeed, the two supernatants correspond to two different media, and even if great care was taken that the standard solutions of IgG(FITC) be prepared in the same media, there is still more chance of calibration errors compared to the indirect ELISA method. On the whole, both adsorption methods gave similar surface coverages of IgG on AuNP as measured by the fluorescence-based assays. In contrast, for a still unknown reason, the indirect ELISA method gave an IgG per AuNP of 9.9 for the physisorbed bioconjugate and 6.9 for the chemisorbed bioconjugate.

3.6. Immunoreactivity of IgG adsorbed to AuNP

Finally, the immunoreactivity of IgG physisorbed or chemisorbed to the AuNP was investigated by ELISA with HRP-labelled goat-anti-rabbit IgG [40, 41]. The same assay was also performed with AuNP-BSA conjugate to take into account non specific binding. Overall, AuNP-IgG(FITC) bound 4.6 HRP-anti-IgG per AuNP while AuNP-S-IgG(FITC) bound 3.6 HTP-anti-IgG per AuNP. By comparison, the amount of HRP-anti-IgG bound to AuNP-BSA was negligible. Since on the other hand, the IgG-to-AuNP ratio was equal to 4.3 and 3.9 for AuNP-IgG(FITC) and AuNP-S-IgG(FITC), respectively, we can conclude that the immunoreactivity of the chemisorbed IgG was very similar to that of the physisorbed IgG and that each IgG molecule bound one HRP-anti-IgG in average.

4. CONCLUSIONS

In this paper, we set up a direct, fluorescence-based assay to quantify the amount of immunoglobulin G (IgG) adsorbed on AuNP *via* two different coupling chemistries, i.e. physisorption and chemisorption of thiolated antibody, and we compared its analytical performances with two indirect assays based on fluorescence or ELISA. We found that the direct fluorescence assay of the bioconjugates after dissolution by NaCN gave a more reasonable quantification of IgG surface coverage compared to the other indirect methods based on the difference between added IgG and excess IgG in supernatants. The method of preparation of IgG conjugated AuNP, either by physisorption or by chemisorption, did not influence the final IgG-to-AuNP ratio, according to the direct fluorescence assay. Conversely, more IgG was adsorbed on AuNP *via* physisorption compared to chemisorption as calculated by indirect ELISA. We believe that the direct fluorescence-based method is reliable for quantification of antibody surface coverage on AuNP. This assay can be employed with confidence whatever the conjugation method, and by then it will be useful to assess novel coupling chemistries of antibody to AuNP and the reproducibility of the antibody-AuNP bioconjugation.

ACKNOWLEDGMENTS

This work was supported by the French-Singaporean PHC Merlion programme [grant 5.03.15]. This work was also supported by ANR-FWF programme, project NanoBioSensor [grant ANR-15-CE9-0026-02]. L.Z thanks the Sorbonne Université – NTU Dual Degree PhD programme for scholarship funding.

REFERENCES

[1] D.H. Choi, S.K. Lee, Y.K. Oh, B.W. Bae, S.D. Lee, S. Kim, Y.-B. Shin, M.-G. Kim, A dual gold nanoparticle conjugate-based lateral flow assay (LFA) method for the analysis of troponin I, Biosens. Bioelectron. 25(8) (2010) 1999-2002.

[2] M. Ben Haddada, D. Hu, M. Salmain, L. Zhang, C. Peng, Y. Wang, B. Liedberg, S. Boujday, Gold nanoparticle-based localized surface plasmon immunosensor for staphylococcal enterotoxin A (SEA) detection, Anal. Bioanal. Chem. 409(26) (2017) 6227-6234.

[3] F. Inci, O. Tokel, S. Wang, U.A. Gurkan, S. Tasoglu, D.R. Kuritzkes, U. Demirci, Nanoplasmonic quantitative detection of intact viruses from unprocessed whole blood, ACS Nano 7(6) (2013) 4733-4745.

[4] Y. Uludag, I.E. Tothill, Cancer biomarker detection in serum samples using surface plasmon resonance and quartz crystal microbalance sensors with nanoparticle signal amplification, Anal. Chem. 84(14) (2012) 5898-5904.

[5] X. Liu, Q. Dai, L. Austin, J. Coutts, G. Knowles, J. Zou, H. Chen, Q. Huo, A One-Step Homogeneous Immunoassay for Cancer Biomarker Detection Using Gold Nanoparticle Probes Coupled with Dynamic Light Scattering, J. Am. Chem. Soc. 130(9) (2008) 2780-2782.

[6] B.-Y. Hsieh, Y.-F. Chang, M.-Y. Ng, W.-C. Liu, C.-H. Lin, H.-T. Wu, C. Chou, Localized Surface Plasmon Coupled Fluorescence Fiber-Optic Biosensor with Gold Nanoparticles, Anal. Chem. 79(9) (2007) 3487-3493.

[7] D. Liu, X. Huang, Z. Wang, A. Jin, X. Sun, L. Zhu, F. Wang, Y. Ma, G. Niu, A.R. Hight Walker, X. Chen, Gold Nanoparticle-Based Activatable Probe for Sensing Ultralow Levels of Prostate-Specific Antigen, ACS Nano 7(6) (2013) 5568-5576.

[8] X. Qian, X.H. Peng, D.O. Ansari, Q. Yin-Goen, G.Z. Chen, D.M. Shin, L. Yang, A.N. Young, M.D. Wang, S. Nie, In vivo tumor targeting and spectroscopic detection with surface-enhanced Raman nanoparticle tags, Nat. Biotechnol. 26(1) (2008) 83-90.

[9] Y. Wang, L.J. Tang, J.H. Jiang, Surface-enhanced raman spectroscopy-based, homogeneous, multiplexed immunoassay with antibody-fragments-decorated gold nanoparticles, Anal. Chem. 85(19) (2013) 9213-9220.

[10] A. Lopez, F. Lovato, S. Hwan Oh, Y.H. Lai, S. Filbrun, E.A. Driskell, J.D. Driskell, SERS immunoassay based on the capture and concentration of antigen-assembled gold nanoparticles, Talanta 146 (2016) 388-393.

[11] S. Van Der Heide, D.A. Russell, Optimisation of immuno-gold nanoparticle complexes for antigen detection, J. Colloid Interface Sci. 471 (2016) 127-135.

[12] N.A. Byzova, I.V. Safenkova, E.S. Slutskaya, A.V. Zherdev, B.B. Dzantiev, Less is More: A Comparison of Antibody–Gold Nanoparticle Conjugates of Different Ratios, Bioconjugate Chem. 28(11) (2017) 2737-2746.

[13] N.G. Welch, J.A. Scoble, B.W. Muir, P.J. Pigram, Nature Biotechnology, Biointerphases 12(2) (2017) 02D301-02D301.

[14] S.L. Filbrun, A.B. Filbrun, F.L. Lovato, S.H. Oh, E.A. Driskell, J.D. Driskell, Chemical modification of antibodies enables the formation of stable antibody–gold nanoparticle conjugates for biosensing, Analyst 142(23) (2017) 4456-4467.

[15] P. Ciaurriz, F. Fernández, E. Tellechea, J.F. Moran, A.C. Asensio, Comparison of four functionalization methods of gold nanoparticles for enhancing the enzyme-linked immunosorbent assay (ELISA), Beilstein J. Nanotechnol. 8(1) (2017) 244-253.

[16] S.B. Geng, J. Wu, M.E. Alam, J.S. Schultz, C.D. Dickinson, C.R. Seminer, P.M. Tessier, Facile Preparation of Stable Antibody–Gold Conjugates and Application to Affinity-Capture Self-Interaction Nanoparticle Spectroscopy, Bioconjugate Chem. 27(10) (2016) 2287-2300.

[17] M. Raoof, S.J. Corr, W.D. Kaluarachchi, K.L. Massey, K. Briggs, C. Zhu, M.A. Cheney, L.J. Wilson, S.A. Curley, Stability of antibody-conjugated gold nanoparticles in the endolysosomal nanoenvironment: implications for noninvasive radiofrequency-based cancer therapy, Nanomedicine: NBM 8(7) (2012) 1096-1105.

[18] K. Tripathi, J.D. Driskell, Quantifying Bound and Active Antibodies Conjugated to Gold Nanoparticles: A Comprehensive and Robust Approach To Evaluate Immobilization Chemistry, ACS Omega 3(7) (2018) 8253-8259.

[19] S.L. Filbrun, J.D. Driskell, A fluorescence-based method to directly quantify antibodies immobilized on gold nanoparticles, Analyst 141(12) (2016) 3851-3857.

[20] G.T. Hermanson, Chapter 24 - Preparation of Colloidal Gold-Labeled Proteins, in: G.T. Hermanson (Ed.), Bioconjugate Techniques (Second Edition), Academic Press, New York, 2008, pp. 924-935.

[21] H. Liao, J.H. Hafner, Gold Nanorod Bioconjugates, Chem. Mater. 17(18) (2005) 4636-4641.

[22] S.Y. Liu, J. Horak, M. Holdrich, M. Lammerhofer, Accurate and reliable quantification of the protein surface coverage on protein-functionalized nanoparticles, Anal. Chim. Acta 989 (2017) 29-37.

[23] S. Liu, E. Haller, J. Horak, M. Brandstetter, T. Heuser, M. Lämmerhofer, Protein A-and Protein G-gold nanoparticle bioconjugates as nano-immunoaffinity platform for human IgG depletion in plasma and antibody extraction from cell culture supernatant, Talanta 194 (2019) 664-672.

[24] M. Iarossi, C. Schiattarella, I. Rea, L. De Stefano, R. Fittipaldi, A. Vecchione, R. Velotta, B.D. Ventura, Colorimetric Immunosensor by Aggregation of Photochemically Functionalized Gold Nanoparticles, ACS Omega 3(4) (2018) 3805-3812.

[25] M.J. Pollitt, G. Buckton, R. Piper, S. Brocchini, Measuring antibody coatings on gold nanoparticles by optical spectroscopy, RSC Adv. 5(31) (2015) 24521-24527.

[26] N.C. Bell, C. Minelli, A.G. Shard, Quantitation of IgG protein adsorption to gold nanoparticles using particle size measurement, Anal. Methods 5(18) (2013) 4591-4601.

[27] H. Zhao, P.H. Brown, P. Schuck, On the distribution of protein refractive index increments, Biophys. J. 100(9) (2011) 2309-2317.

[28] J. Vörös, The Density and Refractive Index of Adsorbing Protein Layers, Biophys. J. 87(1) (2004) 553-561.

[29] L.M. Demers, C.A. Mirkin, R.C. Mucic, R.A. Reynolds, R.L. Letsinger, R. Elghanian, G. Viswanadham, A Fluorescence-Based Method for Determining the Surface Coverage and Hybridization Efficiency of Thiol-Capped Oligonucleotides Bound to Gold Thin Films and Nanoparticles, Anal. Chem. 72(22) (2000) 5535-5541.

[30] B.L. Baldock, J.E. Hutchison, UV–Visible Spectroscopy-Based Quantification of Unlabeled DNA Bound to Gold Nanoparticles, Anal. Chem. 88(24) (2016) 12072-12080.

[31] Y. Liu, M.K. Shipton, J. Ryan, E.D. Kaufman, S. Franzen, D.L. Feldheim, Synthesis, stability, and cellular internalization of gold nanoparticles containing mixed peptide− poly (ethylene glycol) monolayers, Anal. Chem. 79(6) (2007) 2221-2229.

[32] J. Slot, H. Geuze, A method to prepare isodisperse colloidal gold sols in the size range 3–17 nm, Ultramicroscopy 15(4) (1984) 383.

[33] G.T. Hermanson, Chapter 1 - Functional Targets, in: G.T. Hermanson (Ed.), Bioconjugate Techniques (Second Edition), Academic Press, New York, 2008, pp. 1-168.

[34] X. Liu, M. Atwater, J. Wang, Q. Huo, Extinction coefficient of gold nanoparticles with different sizes and different capping ligands, Colloids Surf. B 58(1) (2007) 3-7.

[35] P. Chen, N.T. Tran, X. Wen, Q. Xiong, B. Liedberg, Inflection Point of the Localized Surface Plasmon Resonance Peak: A General Method to Improve the Sensitivity, ACS Sens. 2(2) (2017) 235-242.

[36] T. Huang, R.W. Murray, Quenching of [Ru(bpy)3]2+ fluorescence by binding to Au nanoparticles, Langmuir 18(18) (2002) 7077-7081.

[37] S.K. Ghosh, A. Pal, S. Kundu, S. Nath, T. Pal, Fluorescence quenching of 1-methylaminopyrene near gold nanoparticles: Size regime dependence of the small metallic particles, Chem. Phys. Lett. 395(4-6) (2004) 366-372.

[38] N. Catsimpoolas, J.L. Wood, The reaction of cyanide with bovine serum albumin, J. Biol. Chem. 239(12) (1964) 4132-4137.

[39] T.M. Florence, Degradation of protein disulphide bonds in dilute alkali, Biochem. J. 189(3) (1980) 507-520.

[40] E.S. Day, L.R. Bickford, J.H. Slater, N.S. Riggall, R.A. Drezek, J.L. West, Antibody-conjugated gold-gold sulfide nanoparticles as multifunctional agents for imaging and therapy of breast cancer, Int. J. Nanomedicine 5(1) (2010) 445-454.

[41] H. Hinterwirth, G. Stübiger, W. Lindner, M. Lämmerhofer, Gold Nanoparticle-Conjugated Anti-Oxidized Low-Density Lipoprotein Antibodies for Targeted Lipidomics of Oxidative Stress Biomarkers, Anal. Chem. 85(17) (2013) 8376-8384.